Auto-oscillation or Cavitation Surge

In many installations involving a pump that cavitates, violent oscillations in the pressure and flow rate in the entire system occur when the cavitation number is decreased to values at which the head rise across the pump begins to be affected (Braisted and Brennen 1980, Kamijo *et al.* 1977, Sack and Nottage 1965, Natanzon *et al.* 1974, Miller and Gross 1967, Hobson and Marshall 1979). These oscillations can also cause substantial radial forces on the shaft of the order of 20% of the axial thrust (Rosenmann 1965). In the past, this surge phenomenon has commonly been termed *auto-oscillation* though, in more recent times, it has been given the more appropriate name of *cavitation surge*. It can lead to very large flow rate and pressure fluctuations in the system. In boiler feed systems, discharge pressure oscillations with amplitudes as high as 14 *bar* have been reported informally. It is a genuinely dynamic instability in the sense described in the last section, for it occurs when the slope of the pump head rise/flow rate curve is still strongly negative. Another characteristic of cavitation surge is that it appears to occur more readily when the inducer is more heavily loaded; in other words at lower flow coefficients. These are also the circumstances under which backflow will occur. Indeed, Badowski (1969) puts forward the hypothesis that the dynamics of the backflow are responsible for cavitating inducer instability. Further evidence of this connection is provided by Hartmann and Soltis (1960) but with an atypical inducer that has 19 blades. It is certainly the case that the limit cycle associated with a strong cavitation surge appears to involve large periodic oscillations in the backflow. Consequently, it would seem that any nonlinear model purporting to predict the magnitude of cavitation surge should incorporate the dynamics of the backflow. While most of the detailed investigations have focussed on axial pumps and inducers, Yamamoto (1991) has observed and investigated cavitation surge occurring in cavitating centrifugal pumps. He also noted the important role played by the backflow in the dynamics of the cavitation surge.

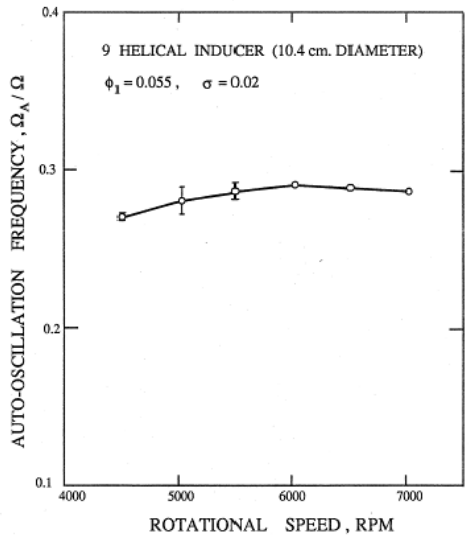

Figure 1: Data from Braisted and Brennen (1980) on the ratio of the cavitation surge frequency to the shaft frequency as a function of the latter for a 9° helical inducer operating at a cavitation number of 0.02 and a flow coefficient of 0.055.

Unlike compressor surge, the frequency of cavitation surge, Ω_A, usually scales with the shaft speed of the pump. Figure 1 (from Braisted and Brennen 1980) demonstrates this by plotting Ω_A/Ω against the shaft *rpm* ($60\Omega/2\pi$) for a particular helical inducer. Figure 2 shows how this reduced cavitation surge frequency,

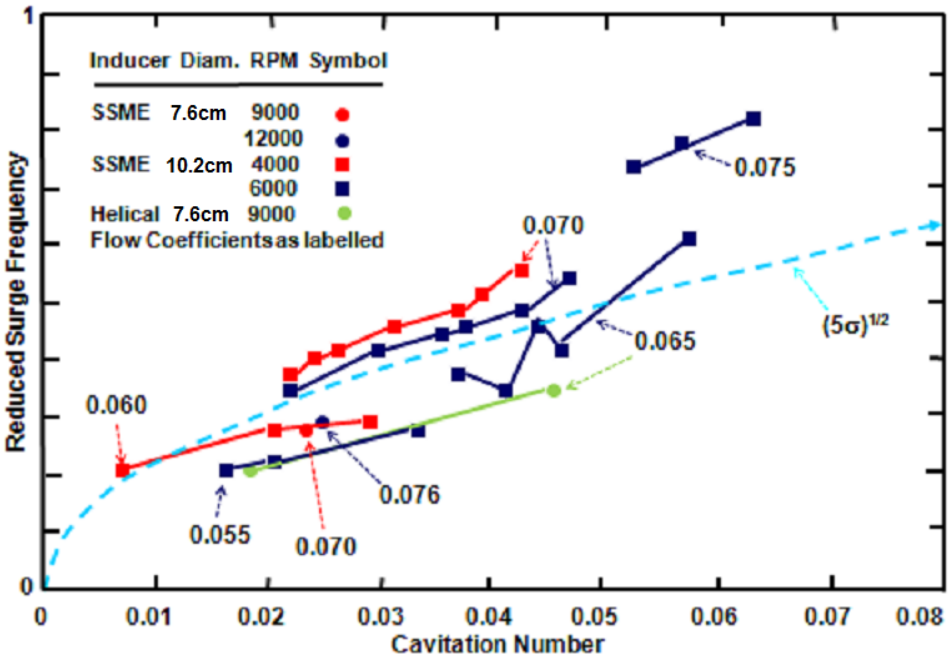

Figure 2: Data from Braisted and Brennen (1980) on the ratio of the frequency of cavitation surge to the frequency of shaft rotation for several inducers: SSME Low Pressure LOX Pump models: 7.62 *cm* diameter: $\times$ (9000 *rpm*) and $+$ (12000 *rpm*), 10.2 *cm* diameter: $\circ$ (4000 *rpm*) and $\Box$ (6000 *rpm*); 9° helical inducers: 7.58 *cm* diameter: $*$ (9000 *rpm*): 10.4 *cm* diameter: $\bigtriangledown$ (with suction line flow straightener) and $\bigtriangleup$ (without suction line flow straightener). The flow coefficients, ϕ_1, are as labelled.

Ω_A/Ω, varies with flow coefficient, ϕ, cavitation number, σ, and impeller geometry. It is evident that the expression

$$\Omega_A/\Omega = (5\sigma)^{\frac{1}{2}} \tag{Mbfg1}$$

provides a good estimate of the cavitation surge frequency. This *natural frequency of a cavitating pump* has a reasonable explanation as follows. Almost any appropriate dynamic model for a cavitating inducer or pump that includes both the primarily non-cavitating main throughflow and the cavitating tip-clearance backflow will include both the pump inertance, L, and the cavitation compliance, C. Thus it will almost inevitably exhibit a natural frequency, Ω_P, given by

$$\Omega_P \;=\; \frac{1}{(LC)^{\frac{1}{2}}} \tag{1}$$

Using the data for the SSME LOX inducer from Section (Nrq) L and C can be approximated by

$$L \;\approx\; \frac{10}{R_t} \quad \text{and} \quad C \;\approx\; \frac{0.05R_t}{\sigma\Omega^2} \tag{2}$$

so that, substituting into equation 1,

$$\frac{\Omega_P}{\Omega} \;\approx\; (2\sigma)^{\frac{1}{2}} \quad \text{or} \quad \Omega'_P \;\approx\; \frac{\Omega_P h}{U_t} \;\approx\; (5\sigma)^{\frac{1}{2}} \tag{3}$$

This is precisely the observed surge frequency proposed empirically by Braisted and Brennen (1980) and shown in figure 2. Indeed the data of figure 2 displays further detail of this cavitating pump property, namely a manifest trend for the frequency to decrease somewhat with flow coefficient. This is most likely the result of an increasing volume of cavitation and increasing compliance as the blades are loaded up at lower flow coefficients. It is important to emphasize that this does not necessarily mean that the major

system instability oscillations occur at this frequency. The study of Hori and Brennen (2011) shows that major instabilities or resonances can occur when this natural frequency for a cavitating pump coincides with other system frequencies such as an organ pipe mode in a suction or discharge tube.

Some data from Yamamoto (1991) on the frequencies of cavitation surge in a centrifugal pump are presented in figure 3. This data exhibits a dependence on the length of the suction pipe that reinforces the understanding of cavitation surge as a system instability. The figure also shows the limits of instability observed by Yamamoto; these are unusual in that there appear to be two separate regions or zones of instability. Finally, it is clear that the data of figures 2 and 3 show a similar dependence of the cavitation surge frequency on the cavitation number, σ, though the magnitudes of σ differ considerably. However, it is likely that the relative sizes of the cavities are similiar in the two cases, and therefore that the correlation between the cavitation surge frequency and the relative cavity size might be closer than the correlation with cavitation number.

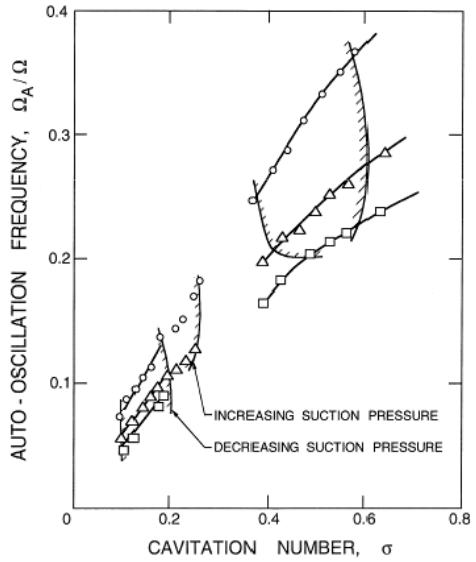

Figure 3: Data from Yamamoto (1991) on the ratio of the frequency of cavitation surge to the frequency of shaft rotation for a centrifugal pump. Data is shown for three different lengths of suction pipe: $\circ$ (2.7 m), $\triangle$ (4.9 m) and $\square$ (7.1 m). Regions of instability are indicated by the hatched lines.

As previously stated, cavitation surge occurs when the region of head loss is approached as the cavitation number is decreased. Figure 4 provides an example of the limits of cavitation surge taken from the work of Braisted and Brennen (1980). However, since the onset is even more dependent than the cavitation surge frequency on the detailed dynamic characteristics of the system, it would not even be wise to quote any approximate guideline for onset. Our current understanding is that the methodologies of Section (Bnca) and (Nrc) are essential for any prediction of cavitation surge.

It should be noted that Section (Nrc) describes linear perturbation models that can predict the limits of oscillation but not the amplitude of the oscillation once it occurs. There do not appear to be any accepted analytical models that can make this important prediction. Furthermore, the energy dissipated in the large amplitude oscillations within the pump can lead to a major change in the mean (time averaged) performance of the pump. One example of the effect of cavitation surge on the head rise across a cavitating inducer is shown in figure 5 (from Braisted and Brennen 1980) which contains cavitation performance curves for three flow coefficients. The sequence of events leading to these results was as follows. For each flow rate, the cavitation number was decreased until the onset of cavitation surge at the point labelled A,

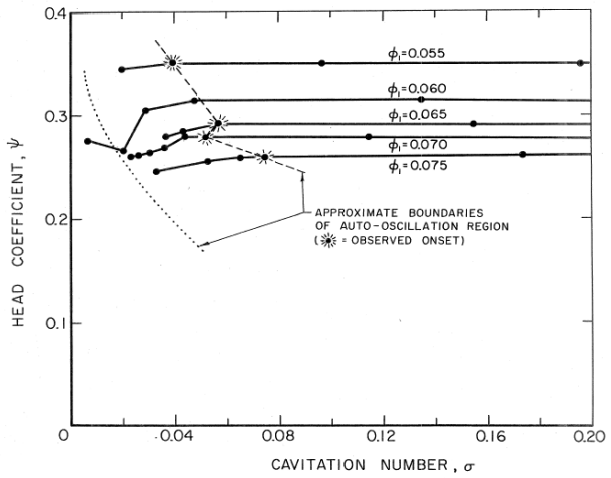

Figure 4: Cavitation performance of the SSME low pressure LOX pump model, Impeller IV, showing the onset and approximate desinence of the cavitation surge at 6000 *rpm* (from Braisted and Brennen 1980).

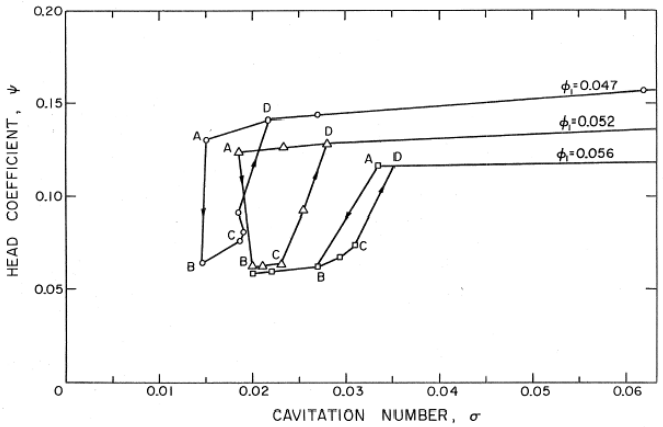

Figure 5: Data from a helical inducer illustrating the decrease in head with the onset of cavitation surge ($A \rightarrow B$) and the cavitation surge hysteresis occurring with subsequent increase in σ (from Braisted and Brennen 1980).

when the head immediately dropped to the point B (an unavoidable change in the pump inlet pressure and therefore in σ would often occur at the same time). Increasing the cavitation number again would not immediately eliminate the cavitation surge. Instead the oscillations would persist until the cavitation number was raised to the value at the point C where the disappearance of cavitation surge would cause recovery to the point D. This set of experiments demonstrate (i) that under cavitation surge conditions (B, C) the head rise across this particular inducer was about half of the head rise without cavitation surge (A, D) and (ii) that a significant cavitation surge hysteresis exists in which the cavitation surge inception and desinence cavitation numbers can be significantly different. Neither of these nonlinear effects can be predicted by the frequency domain methods of Sections (Bnca) and (Nrc). In other inducers, the drop in head with the onset of cavitation surge is not as large as in figure 5 but it is still present; it has also been reported by Rosenmann (1965). This effect may account for the somewhat jagged form of the cavitation characteristic as breakdown is approached.